Indian Journal of Pure & Applied Physics
Vol. 63, July 2025, pp. 607-611
10.56042/ijpap.v63i7.17311

Effect of Oxidation Time on Structural and Morphological Properties of Nickel Thin Films Synthesized by Electron Beam Evaporation Technique

Minakshi[a], Kirti Nanda[b], Dimple[a] & Devendra Mohan[a*]

[a]Department of Physics, Guru Jambheshwar University of Science & Technology, Hisar 125 001, India

[b]Department of Physics, Indian Institute of Technology, Guwahati 781 039, India

Received: 20 February 2025; accepted: 27 May 2025

Nickel thin films were prepared with a simple electron beam evaporation technique. After deposition, the films were oxidized for 1 and 2 h at 4000 °C temperature. The oxidation effect on the structural and morphological properties is discussed. Glancing angle X-ray diffraction data indicated the cubic and hexagonal phase of the prepared samples with space group Fm-3m and P(0) respectively. The FESEM images confirmed the nanostructured surface with closely packed grains. EDX analysis confirmed the presence of constituent elements in the prepared samples. Raman spectroscopy was carried out to study the vibrational modes. The multi-phases found in XRD can extend the spectral range of nonlinear optical effects, making the material suitable for ultrafast photonics and laser applications.

Keywords: Electron beam evaporation, XRD, Raman, FESEM, Laser, Photonics

1 Introduction

Oxide-based thin film technology has played a crucial role in advancing semiconductor devices. Transparent conducting oxides have attracted significant interest due to their ability to balance electrical conductivity with optical transparency. Some of the most widely used TCO materials include copper oxide, zinc oxide, tin oxide, and nickel oxide among others[1-3]. These materials are valued for their versatility and potential applications in optoelectronic devices. Research on oxide materials is becoming increasingly significant due to their diverse functionalities, with many modern electronic devices depending on them. Most metal oxide semiconductors exhibit n-type conductivity and possess stable electrical properties. However, there is a noticeable gap in research focusing on p-type materials, which could complement n-type semiconductors. The limited performance of p-type semiconductors has restricted their potential in transparent device applications. Therefore, improving the efficiency of p-type oxide semiconductors is essential for advancing microelectronic devices[4-5].

Nickel Oxide (NiO) is one of the most studied transparent semiconducting oxides due to its distinctive properties, having p-type conductivity, magnetic storage potential, gas sensing capabilities, and efficient hole transport. Additionally, NiO is a semiconductor with a wide energy band gap, with its band gap energy (Eg) varying between 3.2 and 3.6 eV. Structurally, it features a cubic and hexagonal arrangement, resembling the rock salt structure, which contributes to its high crystallinity[6]. P-type semiconductor thin films are essential for various optoelectronic applications that rely on efficient hole injection. These materials play a crucial role in enhancing the performance of devices by facilitating charge transport and improving overall functionality[7]. Nickel oxide stands out due to its remarkable durability and electrochemical stability, making it a reliable material for various applications. Its cost-effectiveness further enhances its appeal. Additionally, NiO is considered a promising ion storage material due to its excellent cyclic stability. It also offers a broad optical density range, making it suitable for optical applications. Another key advantage is its versatility in fabrication, as it can be produced using multiple techniques, adding to its practical significance in advanced technologies[8]. Several deposition techniques exist to deposit NiO thin films[9-13]. This work aims to explore the structural, morphological and vibrational study of prepared thin films at different oxidation times prepared by Electron beam evaporation technique Fig. 1.

*Corresponding author: E-mail: vand66@yahoo.com

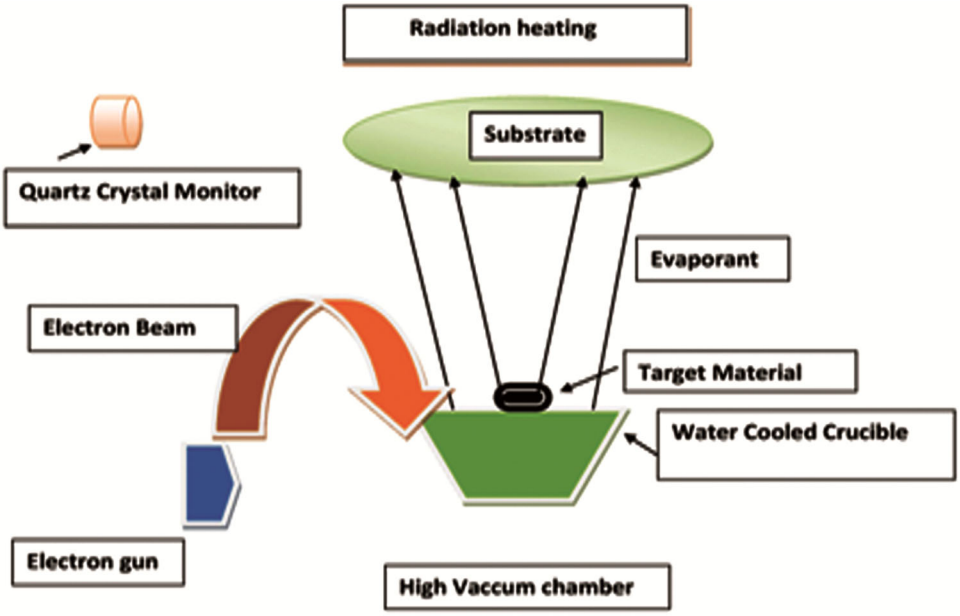

Fig. 1 — Schematic Diagram of Electron Beam Evaporation technique

2 Experimental Details

Nickel oxide thin films were synthesized by a two-step process. Initially, high-purity nickel was deposited onto glass substrates using the electron beam evaporation technique under high-vacuum conditions. Following the deposition, the nickel films underwent thermal oxidation at a temperature of 400°C for durations of 1 h and 2 h in an air atmosphere. To investigate the impact of oxidation temperature and duration on the growth of nickel oxide nanostructures, various characterization techniques were employed. These analyses provided insights into the structural, and morphological properties of the resulting NiO films, helping to understand the effect of oxidation parameters on film quality and material characteristics. More details of the various experimental steps are discussed as follows.

2.1 Ni Thin Film Preparation

Here microscopic glass slides were utilized as substrate. Before starting the deposition microscopic glass was systematically cleaned using acetone, isopropanol, and ethanol then dried in the oven. After ensuring that slides are properly cleaned it is mounted on a substrate holder and placed inside the vacuum chamber. Firstly, the high vacuum was created (~10-5 bar) and then electrons were electrically accelerated using high voltage (~4.5 keV) so that upon striking the Ni target it could easily evaporate. Once the deposition started, it was carefully controlled using the emission current (~mA). For the estimation of the deposition rate, a quartz crystal thickness monitor was used. QCM vibrates at a particular resonance frequency and whenever nickel deposition increases this resonance frequency decreases. This change in frequency was directly related to the mass of nickel deposited onto QCM. So it gives us an idea about the deposition rate and thickness of film deposited on the substrate.

2.2 Ni Film Oxidation

For the thermal oxidation of Ni film, a muffle furnace was utilized to oxidize the Ni films. Nickel-deposited glass slides were placed inside the furnace and thermally oxidized at temperatures (400°C) for 1&2 hours duration at air ambient conditions. When oxygen molecules get sufficient thermal energy they can diffuse into the nickel film. Whenever sufficient time is given to oxygen molecules, they can diffuse deep inside the nickel film and transform the metal phase into a metal oxide phase. To maintain the crystalline quality of the grown nickel oxide nanostructures, slow heating as well as slow cooling process was used.

3 Characterization

The structural phases of the NiO thin films were analyzed using a Rigaku tabletop Miniflex-I X-ray

Table 1 — Calculated values of FWHM(β) ,Crystallite size(D), lattice strain(∈) and dislocation density(δ)of Nickel oxide thin films of (101)plane

Oxidation time	2$\boldsymbol{\theta}$	FWHM (deg)	D(nm)	Lattice strain (∈)	δ (lines^{-1} nm^{-2})
1 hr	44.56	0.40084	18.33	0.000717	0.002976
2 hr	44.75	0.39663	18.52	0.000711	0.002916

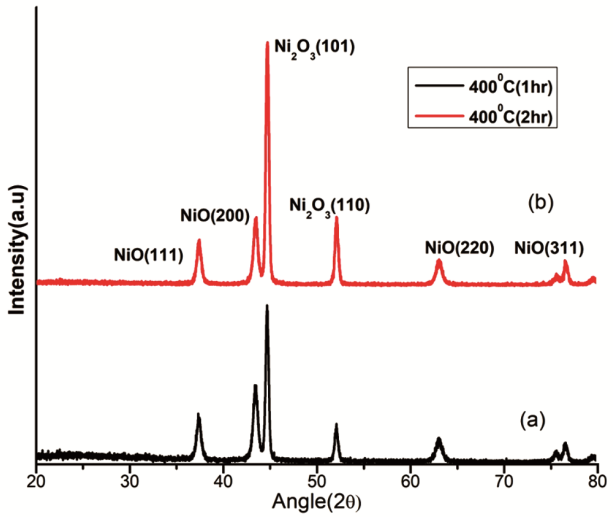

Fig. 2 — GIXRD of temperature treated nickel films at 4000C for (a) 1 h, and (b)2 h

diffractometer within a 2θ range of 10° to 80° at a scanning rate of 2° per minute, with a step size of 0.02°. The apparatus operated at a voltage of 30 kV and a current of 15 mA, utilizing a Cu Kα X-ray source (1.5406 Å). The surface morphology of synthesized samples was examined using a Field Emission Scanning Electron Microscope (7610F PLUS/JEOL). Energy Dispersive X-ray Spectroscopy was used for elemental analysis. To study the modes present in the prepared films, Raman spectroscopy was carried out using a Witec UHTS 300 SMFC system. A laser with a wavelength of 532 nm served as the excitation source for the analysis.

4 Results and Discussion

4.1 Structural Parameters

Figure 2 shows the GIXRD patterns of temperature-treated nickel films. All the peaks appear at around 2$\boldsymbol{\theta}$=37.3,43.4,63.04,76.73,79.22 which were indexed to the(111),(200),(220),(311), and (222) planes corresponding to the cubic phase of NiO having (JCPDS No.04-0835)with space group Fm-3m[14]. Peaks corresponding to 2$\boldsymbol{\theta}$=44.7,52.3 are indexed to (111),(112) planes referring to the Ni2O3 phase of nickel oxide thin films (JCPDS No.14-0481) with space group P(0)[15]. The diffraction patterns show an increase in peak intensity with longer oxidation times. This enhancement can be attributed to improved oxidation kinetics and better crystallinity of the NiO films. The presence of multiple phases in the XRD analysis broadens the spectral range of nonlinear optical responses. This characteristic enhances the material's potential for ultrafast photonics and laser-based applications, making it suitable for high-speed optical switching, frequency conversion, and mode-locked laser systems. A decrease in lattice strain and dislocation density indicates a more ordered and perfect crystalline structure.

The crystallite size was determined using Scherrer's equation(1) for plane (101)[16], lattice strain and dislocation desnity was calculated by Eqs (2) and (3):

$$D = \frac{0.91\lambda}{\beta\cos\theta} \quad \ldots (1)$$

$$\delta = 1/D^2 \quad \ldots (2)$$

$$\in = \frac{\beta}{4\tan\theta} \quad \ldots (3)$$

D is crysttalite size, λ are wavelength of X-ray radiation, β *is* FWHM respectively. The calculated FWHM values, crystallite sizes from Scherrer's equation, lattice strain and dislocation density are listed in Table 1.

4.2 Surface Morphological Study

The surface morphological properties of the NiO films was analyzed through FESEM. Micrographs, presented in Fig. 3(a-b), depict the morphology of NiO films deposited on a glass substrate. The images reveal an increase in porosity between the agglomerated nanograins as the oxidation time increases, suggesting the development of mesoporous films.

4.3 EDX Spectroscopy

The elemental composition of the films deposited on glass substrates was analyzed using Energy Dispersive X-ray Spectroscopy (EDX). Figure 4 confirms the presence of oxygen and nickel in the samples. The atomic percentages of Ni and O are presented in Table 2, indicating that the Ni content is

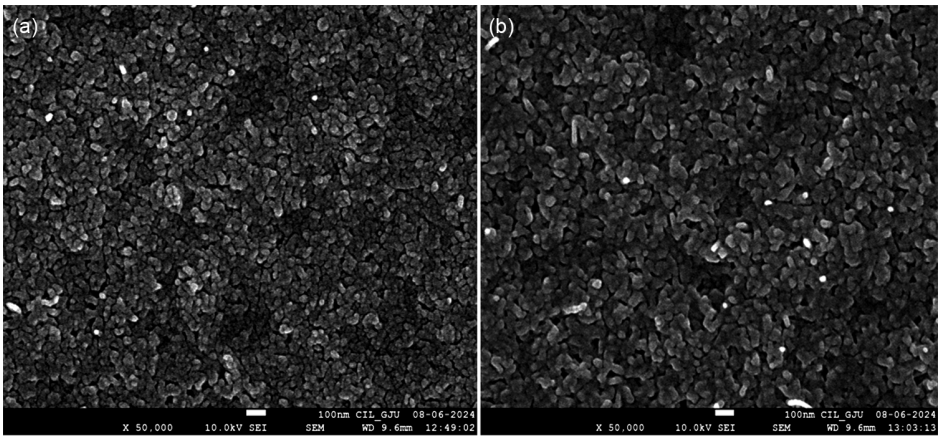

Fig. 3 — FESEM micrograph of thin films oxidized at (a)1hr (b) 2hrs

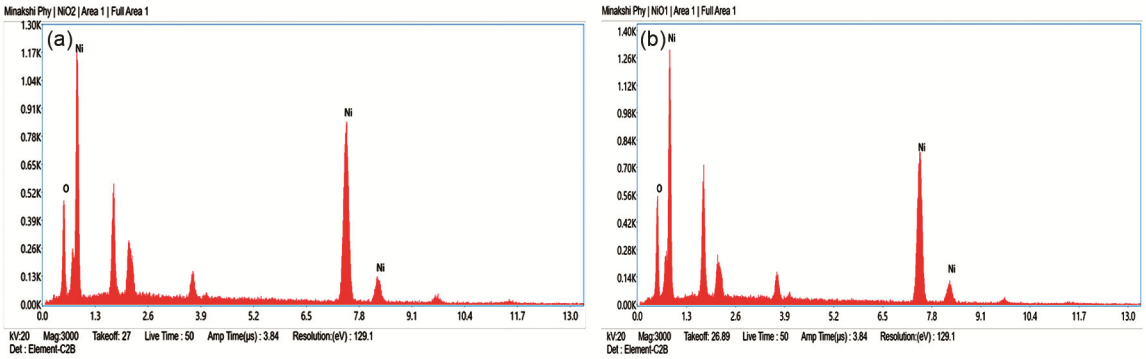

Fig. 4 — EDX analysis of temperature treated films (a) 1 h, and (b) 2 h

Table 2 — Compositional analysis of NiO thin films oxidized at different time

Oxidation time	Element	Atomic (%)	Weight (%)
1 h	Ni	44.7	18
	O	55.3	82
2 h	Ni	49.3	21
	O	50.7	79

higher than that of O in both films. Additional peaks observed in the spectra result from the gold coating applied to the samples. No impurities were detected in the films based on the EDX analysis.

5 Raman Spectroscopy

Raman spectroscopy is an optical technique used to analyze molecular vibrations, enabling the identification of a sample's chemical structure. Figure 5 displays the Raman spectrum of the NiO thin film. The Raman spectrum of the thin film NiO at below ~170cm^{-1} has a vibrational origin[17]. A peak at ~555 cm^{-1} corresponds to the vibrations of Ni-O[18] (one-phonon TO and LO modes). The band

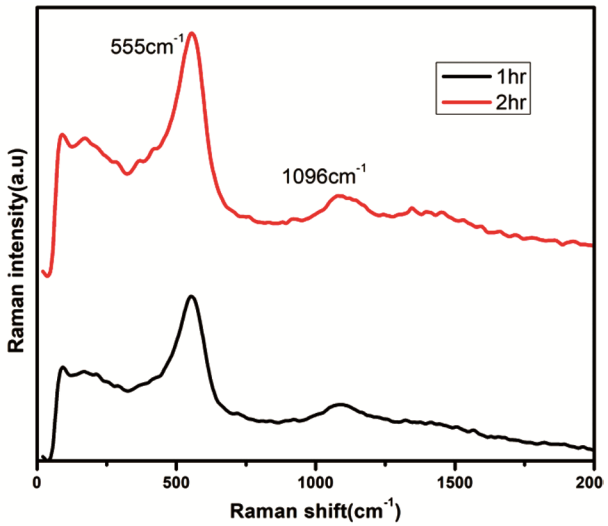

Fig. 5 — Raman spectroscopy of temperature treated films

at ~1,096 cm^{-1} corresponds to 2LO modes which may be due to defects mediated state which could contribute to nonlinear absorption **and** self-focusing effects**.** Longer annealing may reduce defects and enhance the formation of a more

ordered phase which enhances the nonlinear refractive index and a third-order non-linear optical susceptibility result strengthens multi-photon absorption. The Raman intensity increases significantly for the 2-h oxidized sample, indicating an improved crystalline nature.

6 Conclusion

Nickel thin films were synthesized using a straightforward electron beam evaporation technique. Following deposition, the films underwent oxidation at 400°C for durations of 1 and 2 h. The oxidation impact on the structural and morphological characteristics was analyzed. Glancing angle X-ray diffraction revealed the presence of both cubic and hexagonal phases, corresponding to space groups Fm-3m and P(0) respectively. Field Emission Scanning Electron Microscopy images demonstrated a nanostructure surface with densely packed grains. Energy Dispersive X-ray Spectroscopy (EDX) confirmed the presence of essential elements in the samples. Raman spectroscopy was carried out to study the vibrational modes. The multi-phases found in XRD can extend the spectral range of nonlinear optical effects, making the material suitable for ultrafast photonics and laser applications. The samples exhibited a combination of cubic and hexagonal phases, which can be optimized to enhance resistive switching properties, making them promising candidates for next-generation non-volatile memory applications.

Acknowledgments

The authors thank the Central Instrumentation Laboratory, Guru Jambheshwar University of Science & Technology, for facility support.

References

1 Salunkhe P, Muhammed Ali AV & Kekuda D, *Mater Res Express*, (2020)119804.R2.
2 Gobbiner C R, Ali A V M & Kekuda D, *J Mater Sci Mater Electron*, 26 (2015) 9801.
3 Granato D B, Caraveo-Frescas J A, Alshareef H N & Schwingenschlögl U, *Appl Phys Lett*, 102 (2013) 2.
4 Wang Z, Nayak P K, Caraveo-Frescas J A & Alshareef H N, *Adv Mater,* 28 (2016) 3831.
5 Rini P, Mohan R & Parihar V, *Nano structures & Nano-Objects*, 11(2017) 102.
6 Teoh L G & K D, *Materials transactions*, 53 (12) (2012) 2135.
7 Sasi B & Gopchandran K G, *Nanotechnol*, 18 (2007) 115613.
8 K O Ukoba, Eloka-Eboka AC & Inambao F L, *Renew Sustain Energ Rev*, (2017) 1364.
9 Pawar V P, Chougule S, Godse M, Sakhare P, Sen R, Joshi S & Pradeep J, *J Surf Eng Mater Adv Technol*, 1 (2011) 35.
10 Patil P S & Kadam L D, *Appl Surf Sci*, 199 (2002) 211.
11 Porqueras I & Bertran E, *Thin Solid Films,* 41 (2001) 398.
12 Ai L, Fang G, Yuan L, Liu N, Wang M, Li C, Zhang Q, Li Jun & zhong Zhao X, *Appl Surf Sci*, 254 (2008) 2401.
13 Subramanian B, Ibrahim M, Senthilkumar M, Murali V, Vidhya K.R., Sanjeeviraja V S & Jayachandran C, *Phys B Condens Matter*, 403 (2008) 4104.
14 Sasi B & Gopchandran K G, *Nanotechnol*, 18 (2007) 115613
15 Dey S, Bhattacherjee S, Chaudhuri M G & Bose R S, *RSC adv*, 5 (2015) 54717.
16 Emam-Ismail M, El-Hagary M, El-Sherif H M, *Opt Mater*, 112 (2021) 110763.
17 Mironova-Ulmane N, Kuzmin A, Steins I, Grabis J, Slidos I & Pars M, *J Phys: conference Series*, 93 (2007) 012039.